JPET Fast Forward. Published on May 4, 2004 as DOI: 10.1124/jpet.104.068171

Bioactivation of 1,1-Dichloroethylene by CYP2E1 and CYP2F2 in Murine Lung

ANDREA C. SIMMONDS, BURHAN I. GHANAYEM, ASHISH SHARMA, CHRISTOPHER A. REILLY, BRANDIE MILLEN, GAROLD S. YOST, and POH-GEK FORKERT

Department of Anatomy and Cell Biology (A.C.S., A.S, B. M., P.G.F.), Queen's University, Kingston, Ontario, Canada; Laboratory of Pharmacology and Chemistry (B.I.G.), National Institute of Environmental Health Sciences, National Institutes of Health, Research Triangle Park, North Carolina 27709; Department of Pharmacology and Toxicology (C.A.R., G.S.Y.), University of Utah, Salt Lake City, Utah 84112-5820

Running title: Bioactivation of 1,1-Dichloroethylene by CYP2E1 and CYP2F2

Address correspondence to: Dr. Poh-Gek Forkert
Department of Anatomy and Cell Biology
Queen's University
Kingston, Ontario
Canada K7L 3N6
Phone: (613) 533-2854
Fax: (613) 533-2566
E-mail: forkertp@post.queensu.ca

Number of text pages:	34
Number of tables:	1
Figures:	8
References:	39
Number of words in *Abstract*:	248
Number of words in *Introduction*:	748
Number of words in *Discussion*:	1191

ABBREVIATIONS: CHZX, chlorzoxazone; conjugate [C], 2-*S*-glutathionyl acetate; $DASO_2$, diallyl sulfone; DCE, 1,1-dichloroethylene; dH_2O, distilled water; GSH, glutathione; LC/MS, liquid chromatography/mass spectrometry; 5-PIP,5-phenyl-1-pentyne; PNP, *p*-nitrophenol; *S*-Et-GSH, *S*-ethyl glutathione

Section assignment: Toxicology

ABSTRACT

1,1-Dichloroethylene (DCE) exposure evokes lung toxicity with selective damage to bronchiolar Clara cells. Recent *in vitro* studies have implicated CYP2E1 and CYP2F2 in the bioactivation of DCE to 2-*S*-glutathionyl acetate [C], a putative conjugate of DCE epoxide with glutathione. An objective of this study was to test the hypothesis that bioactivation of DCE is catalyzed by both CYP2E1 and CYP2F2 in murine lung. Western blot analysis of lung microsomal proteins from DCE-treated CD-1 mice showed time-dependent loss of immunodetectable CYP2F2 and CYP2E1 protein. Dose-dependent formation of conjugate [C] was observed in the lungs of CD-1 mice treated with DCE (75-225 mg/kg), but was not detected after pretreatment with 5-phenyl-1-pentyne (5-PIP). Treatment of mice with 5-PIP and also with diallyl sulfone ($DASO_2$) significantly inhibited hydroxylation of *p*-nitrophenol (PNP) and chlorzoxazone (CHZX). Incubation of recombinant CYP2F3 (a surrogate for CYP2F2) and recombinant CYP2E1 with PNP and CHZX confirmed that they are substrates for both of the recombinant enzymes. Incubation of the recombinant enzymes with $DASO_2$ or 5-PIP significantly inhibited hydroxylation of both PNP and CHZX. Bronchiolar injury was elicited in CD-1 mice treated with DCE (75 mg/kg), but was abrogated with 5-PIP pretreatment. Bronchiolar toxicity was also manifested in the lungs of CYP2E1-null and wild-type mice treated with DCE (75 mg/kg), but protection ensued after pretreatment with 5-PIP or $DASO_2$. These results showed that bioactivation of DCE in murine lung occurred via the catalytic activities of both CYP2E1 and CYP2F2, and that bioactivation by these enzymes mediated the lung toxicity.

JPET Fast Forward. Published on May 3, 2004 as DOI: 10.1124/jpet.104.068171
This article has not been copyedited and formatted. The final version may differ from this version.

1,1-Dichloroethylene ($Cl_2C=CH_2$) (DCE) is a volatile liquid used mainly for the production of polyvinylidene chloride polymers used principally for food packing and as a barrier coating for paper, cellulose, polypropylene, and other plastics (US EPA 2002). Release of DCE into the environment occurs during its manufacture and use, from the breakdown of polyvinylidene chloride products and from degradation of 1,1,1-trichloroethane, trichloroethylene, tetrachloroethylene and 1,1-dichloroethane. All of these chlorinated hydrocarbons have been identified as environmental contaminants (ATSDR, 1994). Epidemiological studies suggested associations between exposure to DCE in drinking water and birth defects (Goldberg et al., 1990; Bove et al., 1995). However, the drinking water supplies were also contaminated with other chlorinated solvents including trichloroethylene and tetrachloroethylene, and the adverse effects may be associated with cumulative exposure to several chloroethylene compounds.

Exposure of mice to DCE leads to lung toxicity that is manifested as selective damage to Clara cells (Forkert and Reynolds, 1982). These Clara cells contain abundant networks of smooth endoplasmic reticulum and numerous mitochondria, both of which are targets of DCE exposure (Forkert et al., 1986; Martin et al., 2003). The lung toxicity evoked by DCE has been attributed to its bioactivation to reactive intermediates. The initial metabolites formed from DCE are the epoxide, 2,2-dichloroacetaldehyde and 2-chloroacetyl chloride (Dowsley et al., 1995, 1996). The major metabolites detected in microsomal incubations are 2-(*S*-glutathionyl) acetyl glutathione and 2-*S*-glutathionyl acetate (conjugate [C]), both of which are derived from conjugation of glutathione (GSH) with the DCE epoxide (Dowsley et al., 1995, 1996). However, conjugate [C] is the major metabolite generated *in vivo* in mice (Forkert, 1999a, 1999b) and *in vitro* in human lung

and liver (Dowsley et al., 1999). The DCE epoxide is a strong electrophile and an efficient scavenger of GSH, thus rendering this metabolite a plausible candidate for mediating the toxic effects of DCE by depleting GSH and binding to and/or modifying cellular macromolecules (Moussa and Forkert, 1992).

Substantial data have accumulated to demonstrate that CYP2E1 is a major P450 involved in DCE metabolism and formation of conjugate [C] (Lee and Forkert, 1994, 1995; for review, see Forkert, 2001). Decreased amounts of both immunoreactive CYP2E1 and *p*-nitrophenol (PNP) hydroxylation were found in lung microsomes incubated with DCE, whereas neither alterations in CYP2B1 and CYP1A1 protein contents nor in associated enzyme catalytic activities were detected. In other studies, protection from DCE-induced lung toxicity was observed in mice pretreated with the CYP2E1 inhibitor, diallyl sulfone ($DASO_2$) (Forkert et al., 1996a). The protective effect of $DASO_2$ coincided with a 50% decrease in the formation of DCE metabolites including the epoxide (Forkert et al., 1996a; Forkert, 1999a). Formation of DCE metabolites was also inhibited by about 50% in lung microsomes preincubated with a CYP2E1 inhibitory monoclonal antibody before incubation with DCE (Dowsley et al., 1996). These findings indicated that CYP2E1 played an important role in DCE bioactivation but also suggested that other P450 enzymes are involved.

The issue of DCE metabolism by P450 enzymes other than CYP2E1 has been investigated in recent studies (Simmonds et al., submitted)[1]. Our results showed concentration-dependent formation of conjugate [C] from DCE in incubations containing recombinant CYP2F3 (the goat member of the CYP2F family) or recombinant CYP2E1. Formation of conjugate [C] was also detected in lung microsomal incubations in a time-

and concentration-dependent manner. Kinetic analysis revealed that rat and human CYP2E1 generated conjugate [C] at rates greater than or equal to CYP2F3. Likewise, recombinant rat CYP2E1 exhibited much greater affinities than either human CYP2E1 or CYP2F3 (and by analogy the mouse CYP2F2) for the formation of conjugate [C].

In this study, we have tested the hypothesis that lung CYP2F2 and CYP2E1 are both involved in *in vivo* bioactivation of DCE. Immunochemical studies were carried out to determine time-dependent alterations in CYP2F2 and CYP2E1 protein expression in lung microsomes from DCE-treated CD-1 mice. In other studies, mice were treated with $DASO_2$ and 5-phenyl-1-pentyne (5-PIP), both of which inhibit CYP2E1 and/or CYP2F2 (Roberts et al., 1998; Chang et al., 1996), and the inhibitory effects of these compounds on microsomal PNP and chlorzoxazone (CHZX) hydroxylase activities were determined. Kinetic analysis of PNP and CHZX metabolism were also carried out. Histopathologic evaluation was performed to identify alterations in lungs of DCE-treated CD-1, CYP2E1-null and wild-type mice. In addition, mice pretreated with $DASO_2$ and 5-PIP were evaluated for their potential to protect against DCE-induced lung injury. Our results showed that CYP2F2 and CYP2E1 both participate in *in vivo* DCE bioactivation, and that both P450 enzymes play critical roles in producing the Clara cell lesions.

Materials and Methods

Chemicals and Reagents. Chemicals were purchased from suppliers as follows: 1,1-dichloroethylene (> 99% purity), glutathione (Aldrich Chemical Co., Montreal, QC, Canada); glucose-6-phosphate, glucose-6-phosphate dehydrogenase, $NADP^+$, NADPH, monoclonal antibody for β-actin (Sigma Chemical Co., St. Louis, MO); 5-phenyl-1-pentyne (GFS Chemicals Inc., Columbus, OH); low-range SDS-PAGE standards, Immuno-Star™ HRP Substrate Kit (BioRad, Hercules, CA); rat CYP2E1-expressed human β-lymphoblastoid microsomes (Gentest Corp., Woburn, MA); CYP2F1 polyclonal antibody (Genemed, South San Francisco, CA); goat anti-rabbit CYP2E1 polyclonal antibody (Oxford Biomedical, Hornby, ON, Canada); goat anti-mouse IgG conjugated to horseradish peroxidase (BD Biosciences, Mississauga, ON, Canada); rabbit anti-goat-IgG conjugated to horseradish peroxidase (Zymed, South San Francisco, CA); Immunopure IgG Purification Kit (Pierce, Rockford, IL); diallyl sulfone (Colour Your Enzyme, Bath, ON, Canada). All other chemicals and reagents were purchased from standard suppliers.

Treatment of Animals. Female CD-1 mice, weighing 20-25 g, were purchased from Charles River Canada (St. Constant, QC, Canada), maintained on a 12 h light/dark cycle, and were given food (Mouse Diet 5015; PMI Nutrition International, Inc., Brentwood, MO) and water *ad libitum*. They were acclimatized to laboratory conditions for 1 week after arrival. Female wild-type and CYP2E1-null mice were obtained from a colony (mixed 129/Sv and C57BL) developed (Lee et al., 1996) at the National Cancer Institute (Bethesda, MD), and were re-derived and bred at Charles River

Laboratories, Inc. (Wilmington, MA). Female mice, weighing 22-35 g (2-3 months old), were quarantined at the National Institute of Environmental Health Sciences (Research Triangle Park, NC) for 1 week before use in temperature- and humidity-controlled rooms with a 12 h light/dark cycle. National Institutes of Health 31 rodent chow diet and tap water were provided *ad libitum*. All animal care and procedures were performed according to the National Institutes of Health guidelines (NIH, 1985).

Time-course experiments were performed to determine DCE-induced alterations in CYP2F2 and CYP2E1 protein contents. Mice were treated with DCE (75 mg/kg, i.p.) and were sacrificed at the following times after treatment: 5, 15 and 30 min, 1, 24 and 48 h. Control mice were given equivalent volumes of corn-oil and sacrificed at the appropriate times. Microsomes were prepared from lung tissue from these experiments, and were used for Western blot analysis.

To assess the effect of DCE dose on the formation of conjugate [C] *in vivo*, CD-1 mice were treated with 75, 125, 175, 225 mg/kg DCE (i.p.) in corn-oil. For each dose, mice were treated with DCE alone or pretreated with 5-PIP in corn oil (100 mg/kg, i.p.) 1 h before treatment with DCE. The mice were sacrificed 1 h after DCE treatment. Control mice were treated with corn oil or 5-PIP and sacrificed at the appropriate times.

For histopathological studies, CD-1, CYP2E1-null and wild-type mice were treated with DCE (75 mg/kg, i.p.) or pretreated with 5-P1P (100 mg/kg, i.p.) 1 h before treatment with DCE. Additional groups of mice (CYP2E1-null and wild-type) were pretreated with $DASO_2$ (100 mg/kg, p.o.) and then treated with DCE (75 mg/kg, i.p.) 2 h later. In previous studies, protection from DCE-induced Clara cell damage was observed in CD-1 mice pretreated with $DASO_2$ (Forkert et al., 1996a). Therefore, CD-1 mice were not used

in this study for the $DASO_2$ experiments. Control mice were treated with the appropriate vehicle at the appropriate times. All mice were sacrificed 24 h after DCE treatment. Mice were anesthetized with sodium pentobarbital (120 mg/kg, i.p.) before fixation of lung tissues for histopathology.

Preparation of Microsomes. Lungs from 5 mice were pooled for each microsomal sample. Microsomes were prepared and stored according to procedures used in previous studies (Forkert, 1995). Microsomal protein concentrations were determined by the Bradford method using bovine serum albumin as the standard (Bradford, 1976).

Protein Immunoblotting. Protein immunoblotting was performed using procedures described previously (Forkert, 1995), with minor modifications. Blots were prepared initially to confirm the ability of the CYP2F1 antibody to cross-react with the CYP2F2 protein in lung microsomes from untreated CD-1, CYP2E1-null and wild-type mice. For the time-course studies, CYP2F2 and CYP2E1 protein expression was examined in lung microsomes from CD-1 mice treated with DCE. Microsomal proteins were separated by sodium dodecyl sulfate- polyacrylamide gel electrophoresis (SDS-PAGE) on a 8.5% gel and transferred to a membrane. Microsomal proteins from human β-lymphoblastoid cells containing the CYP2F1 insert were included to serve as a positive and a negative control for the CYP2F2 and CYP2E1 blots, respectively. The membrane was incubated for 2 h with a CYP2F1 or a CYP2E1 antibody. The CYP2F1 antibody was generated against a cyclic peptide of 23 amino acids (Nichols et al., 2003), and was IgG purified using an Immunopure IgG Purification Kit (Pierce, Rockford, IL). After rinsing, the membrane was incubated for 1.5 h with a goat anti-rabbit IgG conjugated to horseradish peroxidase (1:8,000). For the CYP2E1 protein blots, rabbit anti-goat-IgG

conjugated to horseradish peroxidase (1:2,500) was used. The protein bands were visualized using chemilluminescence reagents. For time-course experiments, protein loading was assessed by incubation with a monoclonal antibody against β-actin (1:20,000) and a goat anti-mouse IgG horseradish peroxidase antibody (1:20,000). Densitometric analysis of the bands was performed using SigmaGel Gel Analysis Software (Jandel Scientific Software).

Cloning and Expression of CYP2F3. The full-length cDNA of CYP2F3 was cloned into a pCW bacterial expression vector that allows for co-expression of both cytochrome P450 genes and cytochrome P450 oxidoreductase. The CYP2F3/oxidoreductase construct was transformed into competent DH5α bacterial cells. The transformation mixture was spread onto LB plates containing 100 μg/ml ampicillin. Ampicillin-resistant colonies were selected and screened using a restriction digest test. The positive clones were verified by sequence analysis.

The correct bacterial clones were used to inoculate 5 ml of LB broth containing 100 μg/ml ampicillin. The culture was placed into a shaker/incubator and left to grow overnight. This 5 ml culture was then used to inoculate a 500 ml flask of Terrific Broth media containing 100 μg/ml ampicillin. The culture was incubated at 37°C/200 rpm for approximately 2 h when an aliquot of δ-aminolevulinic acid was added (final concentration 0.5 mM). The culture was incubated for 1 h, and then an aliquot of isopropyl-thiogalactopyranoside (IPTG) was added (final concentration 1 mM). Upon induction with IPTG, the rotation speed was decreased to 110 rpm and the temperature was reduced to 30°C. The culture was allowed to incubate for an additional 16 h before the bacterial cells were harvested.

Preparation of Bacterial Membranes. The bacterial membranes were prepared using the method established by Guengerich et al. (1996). The bacterial cell pellets were resuspended in 100 mM tris-acetate buffer (pH 7.6) containing 500 mM sucrose and 0.5 mM EDTA. The suspension was diluted with an equal volume of water containing 0.10 mg/ml of lysozyme, and gently shaken for 30 min to hydrolyze the outer bacterial membrane. The resulting spheroplasts were pelleted at 4000 *g* for 10 min and then resuspended in 100 mM potassium phosphate buffer (pH 7.4) containing 6 mM magnesium acetate, 20% glycerol (v/v) and 0.10 mM dithiothreitol. Protease inhibitors (1 mM phenylmethylsulfonylfluoride, 2 μM leupeptin, 10 μM bestatin and 0.04 U/ml aprotinin) were then added. The cells were lysed with two 20-second sonicator bursts (Branson Sonic Power, Danbury, CT) at 70% power. The lysate was subjected to centrifugation at 10,000 *g* for 10 min and the resulting supernatant was then spun at 100,000 *g* for 60 min. The membrane pellet was resuspended in 50 mM tris-acetate buffer (pH 7.6) containing 0.25 mM EDTA and 250 mM sucrose, and was stored at -70°C until further use.

Preparation of Analytical Standards. The analytical standards for conjugate [C] and *S*-Et-GSH, the internal standard used for quantitative LC/MS analysis of conjugate [C], were prepared by dissolving 10 mg of each compound in 1 ml dH_2O. Stock standards were prepared by serial dilution. All standards were stored at -20^{o} C and protected from light. Quality control samples used to verify the quantitative accuracy of the unknown samples were prepared at concentrations of 50 ng/ml, 1 μg/ml and 20 μg/ml in dH_2O.

Quantitative Analysis of Conjugate [C] by LC/MS. Sample analysis was performed using a Hewlett-Packard Series 1100 LC/MSD (Agilent Technologies, Palo Alto, CA). Samples were diluted 10-fold in dH_2O containing 5 μg/ml *S*-Et-GSH, and analyzed by LC/MS. Liquid chromatographic separation of conjugate [C] and the internal standard (*S*-Et-GSH) was achieved using an Inertsil ODS-3 (100 x 3.0 mm, 3 μm particle size) reversed-phase HPLC column (MetaChem Technologies, Torrance, CA, USA). A stepwise gradient of 0.1% (v/v) formic acid in dH_2O and methanol was used for separation. The column was equilibrated with 100% 0.1% (v/v) formic acid at 25°C with a flow rate of 0.25 ml/min. The mobile phase was maintained at this composition for 3.75 min followed by a linear increase in the concentration of methanol to 25% from 3.75 – 4.00 min. The concentration of methanol was maintained at 25% for 3.90 min and returned to its initial conditions of 100% 0.1% (v/v) formic acid between 7.90- 8.00 min. The duration of the assay was 10.50 min. A 3.50 min time delay between samples was included to ensure proper re-equilibration of the LC column. The auto-sampler injection volume was set at 20 μl and was maintained at room temperature. Under these conditions, conjugate [C] eluted at 4.7 min, while *S*-Et-GSH eluted at 8.3 min.

The mass spectrometer was equipped with an electrospray ionization (ESI) source and was operated in selected-ion monitoring (SIM) mode. The $[M+H]^+$ ions produced from conjugate [C] and *S*-Et-GSH were *m/z* 366 and *m/z* 336, respectively. However, the $[M\text{-}Glu]^+$ ion of conjugate [C] at *m/z* 237 and the $[M\text{-}Glu,\text{-}H_2O]^+$ ion of *S*-Et-GSH at *m/z* 190 were used for quantitative analysis in order to decrease the background MS signals from contaminating substances. The MS conditions were optimized for detection of conjugate [C] and *S*-Et-GSH and were as follows: fragmenter, 100 V; capillary voltage,

2500 V; gas temperature (Nitrogen), 350^{o}C at 10 L/min; and nebulizer pressure, 25 psig. Integration and quantification of the chromatographic peaks were performed using the HP Chemstation software package (revision A.06.03) (Agilent Technologies, Palo Alto, CA, USA). Determination of the concentration of conjugate [C] in the samples was achieved using a standard curve (0 – 25 μg/mL). The standard curve was fit with a quadratic equation weighted $1/Y^2$, where *y* was the peak area ratio of analyte to internal standard and *x* was the concentration of analyte. Calibration curves constructed in this manner exhibited a correlation coefficient (r^2) > 0.998.

Formation of Conjugate [C] in Cytosol. Cytosolic fractions were isolated from the lungs of CD-1 mice in the dose-dependent experiments. Lung tissue from 5 mice was pooled for each sample of cytosol and was prepared as described (Forkert, 1999a). Precipitation and removal of proteins in the cytosol were achieved by centrifugation for 30 min at 100,000 *g*. Cytosolic samples were analyzed by LC/MS for conjugate [C].

PNP Hydroxylation. Hydroxylation of PNP was determined in lung microsomes from control mice and mice treated with $DASO_2$ (100 mg/kg, p.o.) or 5-PIP (100 mg/kg, i.p.). Reaction mixtures in a final volume of 250 μl consisted of lung microsomes (0.5 mg of protein), NADPH (1.5 mM) and potassium phosphate buffer (100 mM), pH 6.8, containing ascorbic acid (0.1 M). After preincubation for 3 min at 37^{o}C, PNP (1 mM) was added, and the incubations were continued for an additional 10 min. Microsomal proteins were precipitated with perchloric acid (70%) and removed by centrifugation. Formation of 4-nitrocatechol was determined in the supernatant fraction by HPLC analysis, using the method described previously (Duescher and Elfarra, 1993), with modifications Samples (100 μl) were analyzed with a reversed-phase C_{18} column (5 μm,

4.6 x 250 mm; Beckman Ultrasphere ODS). The isocratic mobile phase was 25% acetonitrile: 75% H_2O:0.1% trifluoroacetic acid at a flow rate of 1.5 ml/min. The column effluent was monitored at 345 nm. 4-Nitrocatechol eluted from the column at 4.5 min. Levels of PNP hydroxylase activity was determined by relating absorbance to a standard calibration curve of known amounts of 4-nitrocatechol. The enzyme assay was carried out under conditions of linearity with respect to time and protein concentrations.

PNP hydroxylase activities of recombinant CYP2F3 and recombinant CYP2E1 were also determined, and compared with the activities of both recombinant enzymes incubated with $DASO_2$ or 5-PIP. Reaction mixtures contained recombinant CYP2F3 (100 pmol) or CYP2E1 (25 pmol), $DASO_2$ (1 mM) or 5-PIP (1 mM) and NADPH (2 mM). Incubations were carried out for 60 min following which PNP and NADPH (1.5 mM) was added; concentrations of 5 mM and 1 mM of PNP were used for incubations with recombinant CYP2F3 and CYP2E1, respectively. Hydroxylase activity was then determined as described.

CHZX Hydroxylation. CHZX hydroxylase activity was determined in lung microsomes from control mice and mice treated with $DASO_2$ (100 mg/kg, p.o.) or 5-PIP (100 mg/kg, i.p.). Reaction mixtures in a volume of 250 µl contained microsomal proteins (200 µg), CHZX (250 µM) and an NADPH-regenerating system (15 mM glucose-6-phosphate, 10 mM $MgCl_2$, 2 units/ml glucose-6-phosphate dehydrogenase and 0.88 mM $NADP^+$). Incubations were carried out for 15 min at 37°C. The microsomal proteins were removed by centrifugation. Formation of 6-hydroxychlorzoxazone was determined in the supernatant fraction by HPLC analysis using the method described previously (Lucas et al., 1993), with minor modifications. Samples (100 µl) were

analyzed with a reversed-phase C_{18} column (5 μm, 4.6 x 250 mm, Beckman® Ultrasphere ODS column). The isocratic mobile phase consisted of water:acetonitrile: glacial acetic acid (75: 25: 0.5% v/v) at a flow-rate of 1 ml/min. The column effluent was monitored at 287 nm. 6-Hydroxychlorzoxazone eluted from the column at 5.6 min. Levels of CHZX hydroxylase activity were determined by relating absorbance to a standard calibration curve of known amounts of 6-hydroxychlorzoxazone. The enzyme assay was carried out under conditions of linearity with respect to time and protein concentrations.

CHZX hydroxylase activities of recombinant CYP2F3 and recombinant CYP2E1 were determined and compared with activities of both recombinant enzymes incubated with $DASO_2$ or 5-PIP. Reaction mixtures contained recombinant CYP2F3 (100 pmol) or recombinant CYP2E1 (25 pmol), an NADPH-generating system, $DASO_2$ (1 mM) or 5-PIP (1 mM). Incubations were carried out for 60 min following which CHZX (1.0 mM) was added and hydroxylase activity determined as described.

HPLC analysis for PNP and CHZX hydroxylase activities were performed on a Beckman System Gold Programmable Solvent Module 126 HPLC with a Beckman System Gold Module 168 UV detector. The UV spectra were monitored with a Hewlett Packard model 8452 diode array UV spectrophotometer.

Histopathology. Lungs were fixed by tracheal instillation and vascular perfusion with 4% paraformaldehyde in 0.1 M Sörensen's phosphate buffer (12.0 mM NaH_2PO_4, 69.0 mM Na_2HPO_4), pH 7.4, as described (Forkert, 1995). In the case of CYP2E1-null and wild-type mice, the lungs were fixed by intra-tracheal instillation with 4% paraformaldehyde in 0.1 M Sörensen's phosphate buffer, pH 7.4. The tissues were fixed

overnight and were then processed, paraffin-embedded, and sectioned at 5 μm. Tissue sections were stained with hematoxylin and eosin.

Statistical Analysis. Data were expressed as mean ± S.D. and were analyzed using one-way ANOVA followed by the Tukey test to identify significant differences between experimental groups. Data for the studies with recombinant P450 enzymes were analyzed using the Student's *t*-test. The level of significance was set at $p < 0.05$. The apparent K_m and V_{max} values for the rates of PNP and CHZX hydroxylation were determined by Michaelis-Menten kinetics using GraphPad Prism Version 4 (GraphPad Software, Inc., San Diego, CA).

Results

Western Blot Analysis. Recombinant CYP2F1 baculosomes used as a positive control were recognized by the anti-CYP2F1 antibody as a protein band of about 55.5 kDa. Microsomes from untransfected human β-lymphoblastoid cells were used as the negative control, and a protein band was not observed. The human anti-CYP2F1 antibody cross-reacted with CYP2F2 in lung microsomes from untreated CD-1, CYP2E1-null and wild-type mice. Protein bands of similar molecular mass and immunoreactivities were observed (data not shown).

Immunoblotting for CYP2F2 and CYP2E1 was carried out with lung microsomes from CD-1 mice treated with DCE (75 mg/kg, i.p.) or corn-oil and were sacrificed at various times (5, 15 and 30 min, 1, 24 and 48 h) after treatment. A protein band of about 55.5 kDa was detected in lung microsomal proteins probed with the anti-CYP2F1 antibody, and was similar to the band detected for lymphoblastoid microsomes with the CYP2F1 insert (Fig. 1A). Decreased CYP2F immunoreactivity was observed at 0.5, 1, 24 and 48 h in microsomes isolated from DCE-treated mice, compared with the untreated controls (Fig. 1B). A protein band of about 51 kDa was detected for lung microsomal proteins probed with an anti-CYP2E1 polyclonal antibody (Fig. 1C). The immunoreactivity of CYP2E1 in lung microsomes from DCE-treated mice decreased significantly 15 min, 1, 24 and 48 h after DCE treatment versus that in the untreated control (Fig. 1D). The amount of CYP2E1 protein detected at 30 min post-DCE treatment was also decreased but was not statistically different from the control due to the high degree of variability of the samples. The profiles of time-dependent loss of immunodetectable CYP2F2 and CYP2E1 were virtually identical. In the CYP2E1 blot, a

protein band was not detected for human lymphoblastoid microsomes containing the CYP2F1 insert (negative control) (Fig. 1C). Bands representing β-actin were not detected when lymphoblastoid microsomes containing the CYP2F1 insert was loaded, whereas all other protein bands were visualized (Fig. 1, A and C).

Formation of Conjugate [C] in Lung Cytosol. Using LC/MS analysis, formation of conjugate [C] was determined in lung cytosol from mice treated with DCE (75, 125, 175, 225 mg/kg, i.p.) with or without pretreatment with 5-P1P (100 mg/kg, i.p.). Conjugate [C] was detected in lung cytosol from mice treated with all doses of DCE, and was not detected at any dose in mice pretreated with 5-P1P (Fig. 2).

PNP Hydroxylation. PNP hydroxylase activity was readily detectable in lung microsomes from untreated mice (Fig. 3A). Treatment with $DASO_2$ produced a significant decrease (82%) in the rate of PNP hydroxylation (Fig. 3A). Hydroxylase activity was almost completely abolished (99%) in lung microsomes from mice treated with 5-PIP. Incubation of recombinant CYP2E1 or recombinant CYP2F3 with $DASO_2$ decreased PNP hydroxylase activities by 90 and 70%, respectively (Fig. 4, A and B). Hydroxylase activitities were also decreased in incubations of recombinant CYP2E1 (98%) or recombinant CYP2F3 with 5-PIP (Fig. 4, C and D). Kinetic analysis of the rate of PNP hydroxylation by the recombinant P450 enzymes showed that the K_m for CYP2E1 was 28-fold lower than for CYP2F3; the V_{max} for CYP2E1 was 4-fold higher than for CYP2F3 (Table 1).

CHZX Hydroxylation. CHZX hydroxylase activity was substantial in lung microsomes from untreated mice, and was significantly decreased (60%) in mice treated with $DASO_2$ (Fig. 3B). A greater decrease (90%) in hydroxylase activity was elicited in

mice treated with 5-PIP. Hydroxylase activity was also identified in incubations of recombinant CYP2E1 and recombinant CYP2F3 with CHZX (Fig. 5). Incubation of recombinant CYP2E1 and CYP2F3 with $DASO_2$ decreased hydroxylase activity by 90 and 77%, respectively (Fig. 5, A and B). Similarly, incubation of recombinant CYP2E1 and recombinant CYP2F3 with 5-PIP decreased hydroxylase activity by 99 and 89%, respectively (Fig. 5, C and D). Kinetic analysis showed that the K_m values for CHZX metabolism by recombinant CYP2E1 and recombinant CYP2F3 were similar (Table 1). However, the V_{max} for CHZX metabolism by recombinant CYP2E1 was 4.7-fold greater than for recombinant CYP2F3.

Histopathology. In controls, in which mice were treated with corn oil or 5-P1P, the bronchiolar epithelium exhibited characteristic features with Clara cells displaying protruding apices (Fig. 6, A and B). However, the bronchiolar epithelium and Clara cells in the lungs of DCE-treated mice exhibited cellular disintegration, and cell debris was found within the airway lumen (Fig. 6C). These pathologic alterations elicited by DCE are consistent with those of previous studies (Forkert et al., 1996b). In mice pretreated with 5-P1P, the bronchiolar epithelium and Clara cells appeared normal (Fig. 6D), and were similar in structure to that in control mice (Fig. 6A).

The bronchiolar epithelium and Clara cells in wild-type and CYP2E1-null mice displayed normal characteristics (Figs. 7A and 8A). In both CYP2E1-null and wild-type mice treated with DCE (75 mg/kg, i.p.), the bronchiolar epithelium was severely damaged, with cell debris from exfoliated epithelium appearing within the airway lumen (Figs. 7B and 8B). Pretreatment of CYP2E1-null and wild-type mice with $DASO_2$ protected from DCE-induced toxicity with the bronchiolar epithelium and Clara cells

appearing normal and intact (Figs. 7C and 8C). Mice were also protected from DCE-induced toxicity by pretreatment with 5-PIP (Figs. 7D and 8D). In summary, bronchiolar and Clara cell injury was manifested only in DCE-treated mice that were not subjected to pretreatment with a P450 inhibitor.

Discussion

The susceptibility of the lung to chemically-induced toxicity is ascribed to its capacity for bioactivation of xenobiotics to reactive metabolites due to the high concentrations of cytochrome P450 enzymes residing within the Clara cells (for reviews, see Gram, 1997 and Yost, 1997). The P450 enzymes responsible for the metabolism of several lung toxicants have been identified and characterized. The relative contributions of CYP2B4 and CYP4B1 to the metabolism of 4-ipomeanol in the rabbit have been identified (Wolf et al., 1982). Studies, using recombinant CYP2F enzymes, showed that CYP2F3 and CYP2F1 are responsible for the bioactivation of 3-methylindole in goat and human lung, respectively (Wang et al., 1998; Thornton-Manning et al., 1996). More recent studies, also using recombinant P450 enzymes, have provided evidence to demonstrate that CYP2F2 has an important role in the metabolic activation of 1-nitronaphthalene and naphthalene (Shultz et al., 1999). Previous studies have identified CYP2E1 as having major involvement in DCE metabolism to the epoxide, both of which were co-localized within the target Clara cells (Dowsley et al., 1996; Forkert, 1995; Forkert, 1999a; for review, see Forkert, 2001). However, the role of other P450 enzymes in DCE bioactivation has yet to be affirmed.

In order to obtain evidence to demonstrate the role of CYP2F2 and CYP2E1 in DCE metabolism, time-course studies were carried out to determine the effects of DCE treatment on CYP2E1 and CYP2F2 protein content in lung microsomes (Fig. 1). Loss of immunodetectable CYP2E1 and CYP2F2 first apparent at 0.5 h after DCE treatment was abolished after 24 h. The time-course of the loss of CYP2E1 and CYP2F2 protein are surprisingly similar, suggesting simultaneous metabolism of DCE by CYP2F2 and

CYP2E1. Furthermore, these findings suggested that DCE is converted to a metabolite(s) that modifies CYP2F2 and CYP2E1 and forms protein adducts, leading in part to alteration of the epitopes and rendering them unrecognizable by the CYP2F1 and CYP2E1 antisera. The protein alterations coincided with enzyme inactivation and supported the role of both P450 enzymes in DCE bioactivation. Relevant in this context is the finding that incubation of lung microsomes with DCE produced no alteration in the protein content of CYP2B1, a constitutive lung P450 (Lee and Forkert, 1995).

The results of this study showed that conjugate [C] was formed in mice treated with DCE, but was abolished in mice pretreated with 5-PIP (Fig. 2), a compound reported to be an inhibitor of both CYP2E1 and CYP2F2 (Chang et al., 1996; Roberts et al., 1998). Previous studies have also shown that pretreatment of mice with $DASO_2$, a compound thought to be a CYP2E1 inhibitor, decreased production of the DCE metabolites by about 50% (Forkert et al., 1996a). Furthermore, formation of DCE metabolites was inhibited by about 50% in lung microsomes preincubated with an inhibitory CYP2E1 antibody (Dowsley et al., 1996). More recent studies confirmed that the rate of conjugate [C] formation in CYP2E1-null mice comprised about 60% of the rate in wild-type mice (Simmonds et al., submitted).[1] These findings indicated that DCE metabolism via CYP2E1 generated about one-half of metabolite levels, with the remainder being produced by other P450 enzymes including CYP2F2.

Because of the inhibition of DCE metabolite formation by $DASO_2$ and 5-PIP, it was of interest to determine more definitively the relative amounts of CYP2E1 and CYP2F2 inhibited *in vivo* by these compounds. Hydroxylation of PNP and CHZX are regarded as selective catalytic markers for the CYP2E1 enzyme (Koop, 1986; Yamazaki et al., 1995).

However, Shultz et al. (1999) reported that PNP is also a substrate for recombinant CYP2F2, and its rate of metabolism is close to the rate reported for recombinant CYP2E1 (Chen et al., 1996). In this study, treatment of mice with $DASO_2$ and 5-PIP markedly inhibited the rate of PNP hydroxylation (Fig. 3A). Treatment with $DASO_2$ and 5-PIP also significantly inhibited the rates of CHZX hydroxylation (Fig. 3B). These findings confirmed that both compounds inhibited CYP2E1, but also raised a question as to whether CHZX is a substrate for CYP2F2, in addition to CYP2E1, CYP2C11, CYP1A2, CYP3A1 and CYP3A2 as reported previously (Kobayashi et al., 2002). To obtain data in support of such a possibility, we incubated recombinant CYP2F3 and recombinant CYP2E1 with PNP and CHZX and measured the rate of hydroxylation of these substrates. Our results confirmed that PNP and CHZX are both substrates for recombinant CYP2E1 and CYP2F3 (Figs. 4 and 5). Kinetic analysis revealed that the apparent K_m for the metabolism of CHZX by CYP2F3 and CYP2E1 were similar (Table 1). However, the V_{max} for CYP2E1 was 4.7-fold higher than for CYP2F3 (Table 1). These findings indicated that recombinant CYP2E1 is a more efficient catalyst of CHZX metabolism than recombinant CYP2F3. Furthermore, the catalytic efficiencies of both recombinant CYP2E1 and recombinant CYP2F3 for CHZX metabolism are higher than for PNP: the apparent K_m values for CHZX are lower and apparent V_{max} values are higher for both recombinant enzymes (Table 1). Incubation of recombinant CYP2F3 or recombinant CYP2E1 with $DASO_2$ or 5-PIP inactivated both P450 enzymes, leading to significant inhibition of PNP and CHZX hydroxylase activities (Figs. 4 and 5). Taken together, these findings showed that PNP and CHZX are substrates for both recombinant CYP2E1 and recombinant CYP2F3, albeit with vastly differing affinities. Furthermore,

the findings suggested that the inhibitory effects of $DASO_2$ and 5-PIP are associated with their metabolism by CYP2E1 and CYP2F3, leading to P450 inactivation, deficient DCE metabolite formation and protection from DCE-induced bronchiolar toxicity.

Previous studies have shown that pretreatment of CD-1 mice with $DASO_2$ provided protection from DCE-induced bronchiolar toxicity (Forkert et al., 1996a). This protective effect of $DASO_2$ was attributed to diminished production of DCE metabolites including the epoxide. In this study, pretreatment of CD-1 mice with 5-PIP also protected from DCE-induced bronchiolar toxicity (Fig. 6) analogous to that resulting from $DASO_2$ pretreatment reported previously (Forkert et al., 1996a). This protective effect of 5-PIP coincided with the complete inhibition of conjugate [C] formation in mice pretreated with 5-PIP (Fig. 2). The protection provided by $DASO_2$ and 5-PIP are consistent with our data indicating that formation of conjugate [C] mediated by CYP2F2 and CYP2E1 is inhibited by these two chemicals. Bronchiolar lesions were also observed in the lungs of CYP2E1-null (Fig. 8B) and wild-type (Fig. 7B) mice treated with DCE. Manifestation of cytotoxicity in CYP2E1-null mice indicated that DCE bioactivation catalyzed by P450 enzymes other than CYP2E1 occurs, and likely involves CYP2F2. This observation suggested that DCE metabolism via constitutive CYP2F2 generates amounts of metabolite(s) sufficient for causing bronchiolar damage. Hence, the protection resulting from pretreatment with 5-PIP and $DASO_2$ in CYP2E1-null mice (Figs. 6 and 7, C and D) is in concordance with inhibition of CYP2F2-mediated metabolite formation from DCE.

In summary, the results of this investigation show that bioactivation of DCE in murine lung is catalyzed by CYP2F2 and CYP2E1. Furthermore, $DASO_2$ and 5-PIP inhibited these P450 enzymes as well as DCE metabolite formation and provided

protection from bronchiolar Clara cell damage. We also report the novel finding that CHZX and PNP are both substrates for CYP2F3. In conclusion, the enhanced susceptibility of the lung to DCE-induced toxicity is mediated in part by its bioactivation by CYP2E1 and CYP2F2 within the target Clara cells.

References

ATSDR (Agency for Toxic Substances and Disease Registry) (1994) Toxicological profile for 1,1-dichloroethylene. ATSDR, Atlanta, G.A.

Bove FJ, Fulcomer MC, Klotz JB, Esmart J, Dufficy EM and Savrin JE (1995) Public drinking water contamination and birth outcomes. *Am J Epidemiol* **141:**850-862.

Bradford MM (1976) A rapid and sensitive method for the quantitation of microgram quantities of protein utilizing the principle of protein-dye binding. *Anal Biochem* **72**:248-254.

Chang A, Buckpitt A, Plopper C and Allworth W (1996) Suicide inhibition of CYP2F2, the enzyme responsible for naphthalene (NA) metabolism to a Clara cell toxicant. *Toxicologist* **30:**72.

Chen W, Peter RM, McArdle S, Thummel KE, Sigle RO and Nelson SD (1996) Baculovirus expression and purification of human and rat cytochrome P450 2E1. *Arch Biochem Biophys* **335:**123-130.

Dowsley TF, Forkert PG, Benesch LA and Bolton JL (1995) Reaction of glutathione with the electrophilic metabolites of 1,1-dichloroethylene. *Chem Biol Interact* **95**:227-244.

Dowsley TF, Reid K, Petsikas D, Ulreich JB, Fisher RL and Forkert PG (1999) Cytochrome P-450-dependent bioactivation of 1,1-dichloroethylene to a reactive epoxide in human lung and liver microsomes. *J Pharmacol Exp Ther* **289**:641-648.

Dowsley TF, Ulreich JB, Bolton JL, Park SS and Forkert PG (1996) CYP2E1-dependent bioactivation of 1,1-dichloroethylene in murine lung: formation of reactive intermediates and glutathione conjugates. *Toxicol Appl Pharmacol* **139**:42-48.

Duescher RJ and Elfarra AA (1993) Determination of *p*-nitrophenol hydroxylase activity of rat liver microsomes by high-presssure liquid chromatography. *Anal Biochem* **212:**311-314.

Forkert PG (2001) Mechanisms of 1,1-dichloroethylene-induced cytotoxicity in lung and liver. *Drug Metab Rev* **33:**49-80.

Forkert PG (1995) CYP2E1 is preferentially expressed in Clara cells of murine lung: localization by *in situ* hybridization and immunohistochemical methods. *Am J Respir Cell Mol Biol* **12:**589-596.

Forkert PG (1999a) 1,1-Dichloroethylene-induced Clara cell damage is associated with *in situ* formation of the reactive epoxide. *Am J Respir Cell Mol Biol* **20:** 1310-1318.

Forkert PG (1999b) In vivo formation and localization of 1,1-dichloroethylene epoxide in murine liver: identification of its glutathione conjugate 2-*S*-glutathionyl acetate. *J Pharmacol Exp Ther* **290:**1299-1306.

Forkert PG, Dowsley TF, Lee RP, Hong J-Y and Ulreich JB (1996b) Differential formation of 1,1-dichloroethylene metabolites in the lungs of adult and weanling male and female mice: correlation with severities of bronchiolar cytotoxicity. *J Pharmacol Exp Ther* **279:**1484-1490.

Forkert PG, Lee RP, Dowsley TF, Hong JY and Ulreich JB (1996a) Protection from 1,1-dichloroethylene-induced Clara cell injury by diallyl sulfone, a derivative of garlic. *J Pharmacol Exp Ther* **277:**1665-1671.

Forkert PG and Reynolds ES (1982) 1,1-Dichloroethylene-induced pulmonary injury. *Exp Lung Res* **3:**57-68.

Forkert PG, Stringer V and Troughton KM (1986) Pulmonary toxicity of 1,1-dichloroethylene: correlation of early changes with covalent binding. *Can J Physiol Pharmacol* **64:**12-121.

Goldberg SJ, Lebowitz MD, Graver EJ and Hicks S (1990) An association of human congenital cardiac malformations and drinking water contaminants. *J Am Coll Cardiol* **16:**155-164.

Gram T (1997) Chemically reactive intermediates and pulmonary xenobiotic toxicity. *Pharmcol Rev* **49:**297-341.

Guengerich FP, Martin MV, Guo Z and Chun YJ (1996) Purification of functional recombinant P450s from bacteria. *Methods in Enzymol* **272:**35-44.

Kobayashi K, Urashima K, Shimada N and Chiba K (2002) Substrate specificity for rat cytochrome P450 (CYP) isoforms: screening with cDNA-expressed systems of the rat. *Biochem Pharmacol* **63:**889-896.

Koop DR (1986) Hydroxylation of *p*-nitrophenol by rabbit ethanol-inducible cytochrome P-450 isozyme 3a. *Mol Pharmacol* **29:**399-404.

Lee RP and Forkert PG (1994) In vitro biotransformation of 1,1-dichloroethylene by hepatic cytochrome P-450 2E1 in mice. *J Pharmacol Exp Ther* **270:**371-376.

Lee RP and Forkert PG (1995) Pulmonary CYP2E1 bioactivates 1,1-dichloroethylene in male and female mice. *J Pharmacol Exp Ther* **273:**561-567.

Lee SS, Pineau T, Fernandez-Salguero P and Gonzalez, FJ (1996) Role of CYP2E1 in the hepatotoxicity of acetaminophen *J Biol Chem* **271:**12063-12067.

Lucas D, Berthou F, Girre C, Poitrenaud F and Menez J-F (1993) High-performance liquid chromatographic determination of chlorzoxazone and 6-hydroxychlorzoxazone

in serum: a tool for indirect evaluation of cytochrome P4502E1 activity in humans. *J Chromatogr* **622:**79-86.

Martin EJ, Racz WJ and Forkert PG (2003) Mitochondrial dysfunction is an early manifestation of 1,1-dichloroethylene-induced hepatotoxicity in mice. *J Pharmacol Exp Ther* **304:**121-129.

Moussa M and Forkert PG (1992) 1,1-Dichloroethylene-induced alterations in glutathione and covalent binding in murine lung: morphological, histochemical and biochemical studies. *J Pathol* **166:** 199-207.

Nichols WK, Mehta R, Skordos K, Macé K, Pfeifer AMA, Carr BA, Minko T, Burchiel SW and Yost GS (2003) 3-Methylindole-induced toxicity to human bronchial epithelial cell lines. *Toxicol Sci* **71:** 229-236.

NIH (1985) Guide for the care and use of laboratory animals. U.S. Department of Health and Human Services, Animal Resources Program, Division of Resources, Bethesda, Maryland.

Roberts ES, Alworth WL and Hollenberg PF (1998) Mechanism-based inactivation of cytochromes P450 2E1 and 2B1 by 5-phenyl-1-pentyne. *Arch.Biochem.Biophys.* **354**:295-302.

Shultz MA, Choudary PV and Buckpitt AR (1999) Role of murine cytochrome P-450 2F2 in metabolic activation of naphthalene and metabolism of other xenobiotics. *J Pharmacol Exp Ther* **290:**281-288.

Thornton-Manning J, Appleton ML, Gonzalez FJ and Yost G (1996) Metabolism of 3-methylindole by vaccinia-expressed P450 enzymes: Correlation of 3-methyleneindolenine formation and protein-binding. *J Pharmcol Exp Ther* **276:**21-29.

U.S. EPA (Environmental Protection Agency) (2002) Toxicological review of 1,1-dichloroethylene. In support of summary information on the integrated risk information system (IRIS) (CAS No. 75-35-4; EPA/635/R02/002). Washington, DC.

Wang H, Lanza DL and Yost GS (1998) Cloning and expression of CYP2F3, a cytochrome P450 that bioactivates the selective pneumotoxins 3-methylindole and naphthalene. *Arch Biochem Biophys* **349:**329-340.

Wolf CR, Statham C, McMenamin M, Bend J, Boyd M and Philpot R (1982) The relationship between the catalytic activities of rabbit pulmonary cytochrome P450 isozymes and the lung specific toxicity of the furan derivative, 4-ipomeanol. *Mol Pharmacol* **22:**738-744.

Yamazaki H, Guo Z and Guengerich FP (1995) Selectivity of cytochrome P4502E1 in chlorzoxazone 6-hydroxylation. *Drug Metab Dispos* **23:**438-440.

Yost GS (1997) Selected, nontherapeutic agents, in *Comprehensive Toxicology* (Roth R ed) pp 591-610, Elsevier, New York.

Footnotes

a) This study was supported by Grant MOP 11706 from the Canadian Institutes of Health Research and Grant 014061 from the National Cancer Institute of Canada (to P.G.F.) and United States Public Health Service Grants (HL 13645 and HL60143) from the National Heart, Lung, and Blood Institute (to G.S.Y.). A.S. was supported by postdoctoral fellowships from the Cancer Research Society of Canada and Queen's University Principal's Development Fund.

b) Address correspondence to: Dr. Poh-Gek Forkert
Department of Anatomy and Cell Biology
Queen's University, Kingston
ON, Canada K7L 3N6
E-mail: forkertp@post.queensu.ca

c) [1]Simmonds AC, Reilly CA, Lanza DL, Ghanayem BI, Yost GS, Collins KS, and Forkert PG. Bioactivation of 1,1-dichloroethylene to its epoxide by CYP2E1 AND CYP2F3. Submitted.

Figure Legends

Fig. 1. Western blot analysis for CYP2F2 (A) and CYP2E1 (C) in lung microsomes from mice treated with DCE. The histograms represent relative protein levels of CYP2F2 (B) and CYP2E1 (C), as assessed by densitometric analysis of the protein bands and standardized to β-actin. Mice were treated with DCE (75 mg/kg, i.p.) and were sacrificed at the indicated time-points for isolation of lung microsomes. The first lane of each blot contains protein (15 μg) from human lymphoblastoid cells expressing CYP2F1. For each time-point, the first lane contains protein from control mice, while the second lane contains protein from DCE-treated mice. All lanes were loaded with 40 μg of microsomal protein. Data are expressed as mean ± S.D. *Significantly different from control mice sacrificed at the same time.

Fig. 2. Formation of conjugate [C] in lung cytosol from CD-1 mice treated with DCE. Mice were treated with DCE (75, 125, 175, and 225 mg/kg, i.p.) or were given 5-PIP (100 mg/kg, i.p.) before DCE treatment. Mice were sacrificed 1 h after DCE treatment. Lung cytosol was subjected to LC/MS analysis for determination of conjugate [C] formation. Data are expressed as mean ± S.D.

Fig. 3. Effects of $DASO_2$ and 5-PIP on rates of PNP (A) and CHZX (B) hydroxylation in lung microsomes from CD-1 mice. Mice were treated with $DASO_2$ (100 mg/kg, p.o.), 5-PIP (100 mg/kg, i.p.) or the vehicle, and were sacrificed 3 h after treatment. Rates of PNP and CHZX hydroxylation were determined by HPLC analysis as described under "Materials and Methods". Data are expressed as mean ± S.D. *Significantly different from levels in control. **Significantly different from levels in control and $DASO_2$-treated mice.

Fig. 4. Effects of $DASO_2$ and 5-PIP on rates of PNP hydroxylation by recombinant CYP2E1 (A and C) and CYP2F3 (B and D). Rates of PNP hydroxylation were determined by HPLC analysis as described under "Materials and Methods". Data are expressed as mean ± S.D. The rates of PNP hydroxylation in control incubations were 3.37 ± 0.19 pmol/min/pmol P450. *Significantly different from levels in control incubations.

Fig. 5. Effect of $DASO_2$ and 5-PIP on rates of CHZX hydroxylation by recombinant CYP2E1 (A and C) and CYP2F3 (B and D). Rates of CHZX hydroxylation were determined by HPLC analysis as described under "Materials and Methods". The rates of CHZX hydroxylation in control incubations were 1.91 ± 0.13 nmol/min/pmol P450. *Significantly different from levels in control incubations.

Fig. 6. Lung tissue from CD-1 mice treated with DCE or pretreated with 5-PIP. Mice were treated according to the following regimens: corn-oil (A); 5-P1P (100 mg/kg, i.p.) (B); DCE (75 mg/kg, i.p.) (C); 5-P1P (100 mg/kg, i.p.) 1 h prior to DCE (75 mg/kg, i.p.) treatment (D). Mice were sacrificed 24 h after DCE treatment. Intact Clara cells (*arrowheads*) and normal bronchiolar epithelium are depicted in lung tissue from mice treated with the vehicle (A), 5-PIP (B) or 5-PIP and DCE (D). Cellular debris from exfoliated epithelium (*arrowheads*) is present in the airway lumen in lung tissue from mice treated with only DCE (C). Stain: hematoxylin and eosin. Scale bar: 40 μm.

Fig. 7. Lung tissue from wild-type mice treated with DCE or pretreated with $DASO_2$ or 5-PIP. Mice were treated according to the following regimens: corn oil (A); DCE (75 mg/kg, i.p.) (B); $DASO_2$ (100 mg/kg, p.o.) (C) or 5-PIP (100 mg/kg, i.p.) (D) 1 h before treatment with DCE (75 mg/kg, i.p.). Mice were sacrificed 24 h after DCE treatment.

Intact Clara cells (*arrowheads*) in bronchiolar epithelium of control wild-type mice (A) or wild-type mice pretreated with $DASO_2$ (C) or 5-PIP (D); cellular debris from exfoliated epithelium is observed in the airway lumen of wild-type mice treated with only DCE (*arrowheads*) (B). Stain: hematoxylin and eosin. Scale bar: 40 μm.

Fig. 8. Lung tissue from CYP2E1-null mice treated with DCE or pretreated with $DASO_2$ or 5-PIP. Mice were treated according to the following regimens: corn oil (A); DCE (75 mg/kg, i.p.) (B); $DASO_2$ (100 mg/kg, p.o.) (C) or 5-PIP (100 mg/kg, i.p.) (D) 1 h before treatment with DCE (75 mg/kg, i.p.). Mice were sacrificed 24 h after DCE treatment. Intact Clara cells (*arrowheads*) in bronchiolar epithelium of control CYP2E1-null mice (A) or CYP2E1-null mice pretreated with $DASO_2$ (C) or 5-PIP (D); cellular debris from exfoliated epithelium is observed in the airway lumen of CYP2E1-null mice treated with only DCE (*arrowheads*) (B). Stain: hematoxylin and eosin. Scale bar: 40 μm.

TABLE 1

Kinetic analysis of PNP and CHZX metabolism by recombinant CYP2F3 and recombinant CYP2E1

Reaction mixtures contained recombinant CYP2F3 (100 pmol) or recombinant CYP2E1 (25 pmol), NADPH (2 mM) and PNP or CHZX. In incubations with CYP2E1 and PNP or CHZX, concentrations of substrate used ranged from 0.5 μM - 1.0 mM. In incubations of CYP2F3 with PNP or CHZX, substrate concentrations used ranged from 0.5 - 8.0 mM and 0.5 μM - 1.0 mM, respectively. PNP and CHZX hydroxylase activities were determined by HPLC analysis. Values are mean ± S.D. of triplicate determinations.

Recombinant P450	Substrate	K_m (μM)	V_{max}
CYP2E1	PNP	290 ± 28	8 ± 1 pmol/min/pmol P450
	CHZX	88 ± 3	151 ± 1 nmol/min/pmol P450
CYP2F3	PNP	8335 ± 1212	2 ± 0 pmol/min/pmol P450
	CHZX	77 ± 7	32 ± 1 nmol/min/pmol P450

JPET Fast Forward. Published on May 3, 2004 as DOI: 10.1124/jpet.104.068171
This article has not been copyedited and formatted. The final version may differ from this version.

JPET Fast Forward. Published on May 3, 2004 as DOI: 10.1124/jpet.104.068171
This article has not been copyedited and formatted. The final version may differ from this version.

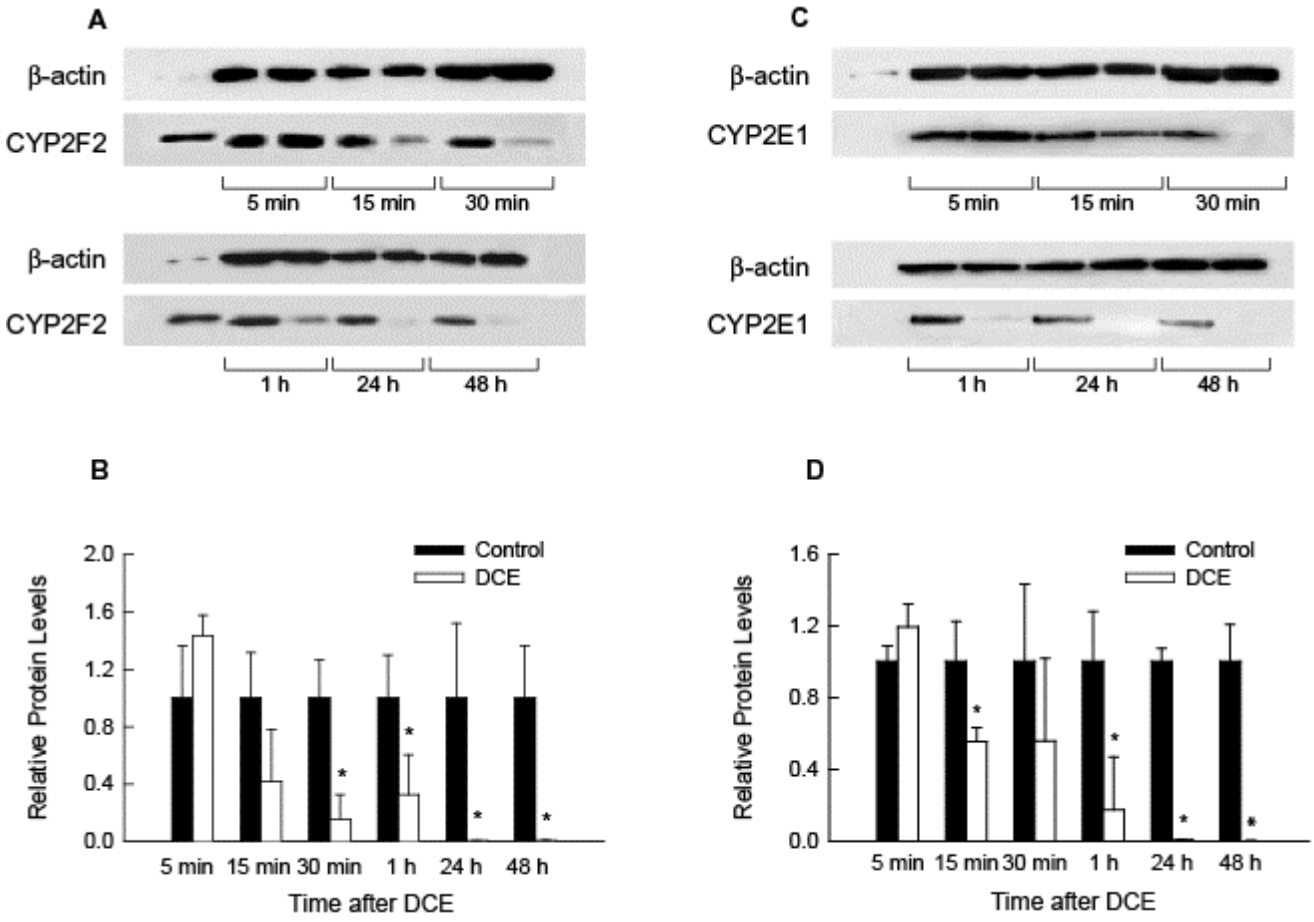

Figure 1

JPET Fast Forward. Published on May 3, 2004 as DOI: 10.1124/jpet.104.068171
This article has not been copyedited and formatted. The final version may differ from this version.

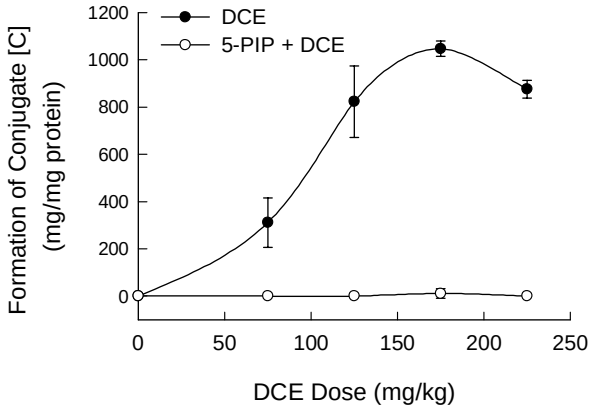

Figure 2

JPET Fast Forward. Published on May 3, 2004 as DOI: 10.1124/jpet.104.068171
This article has not been copyedited and formatted. The final version may differ from this version.

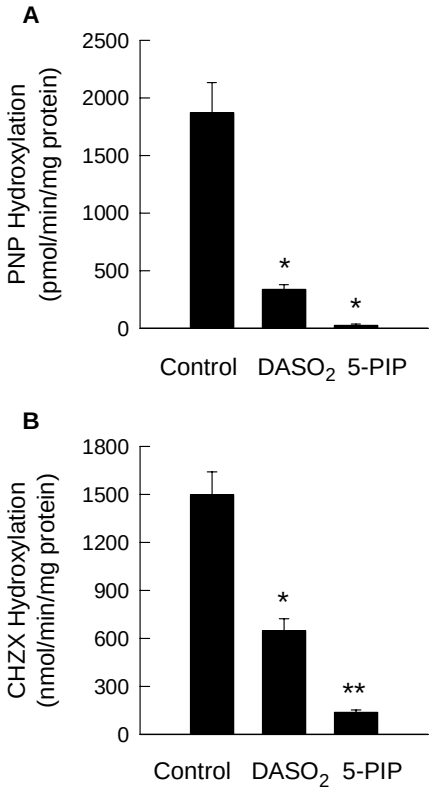

Figure 3

JPET Fast Forward. Published on May 3, 2004 as DOI: 10.1124/jpet.104.068171
This article has not been copyedited and formatted. The final version may differ from this version.

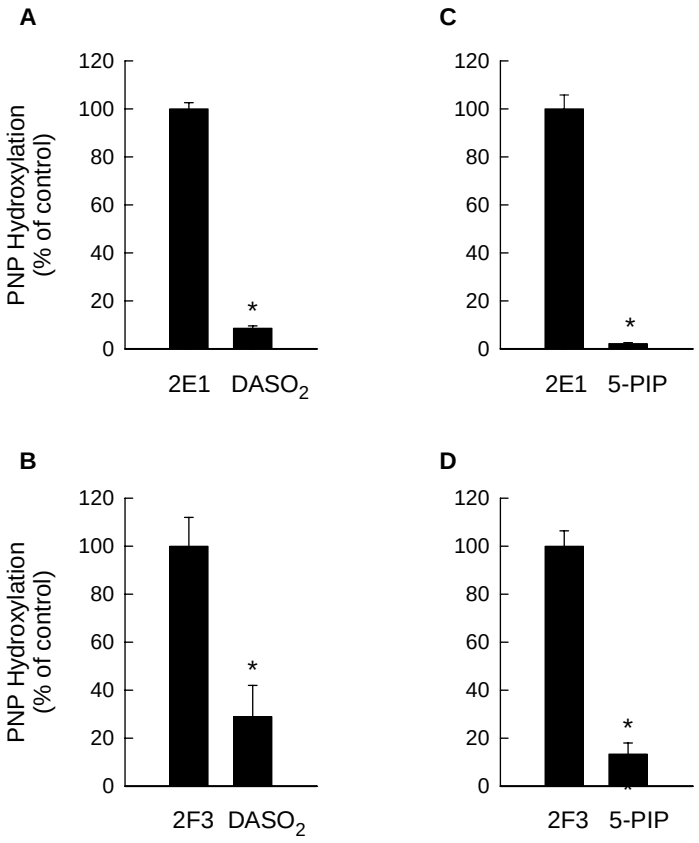

Figure 4

JPET Fast Forward. Published on May 3, 2004 as DOI: 10.1124/jpet.104.068171
This article has not been copyedited and formatted. The final version may differ from this version.

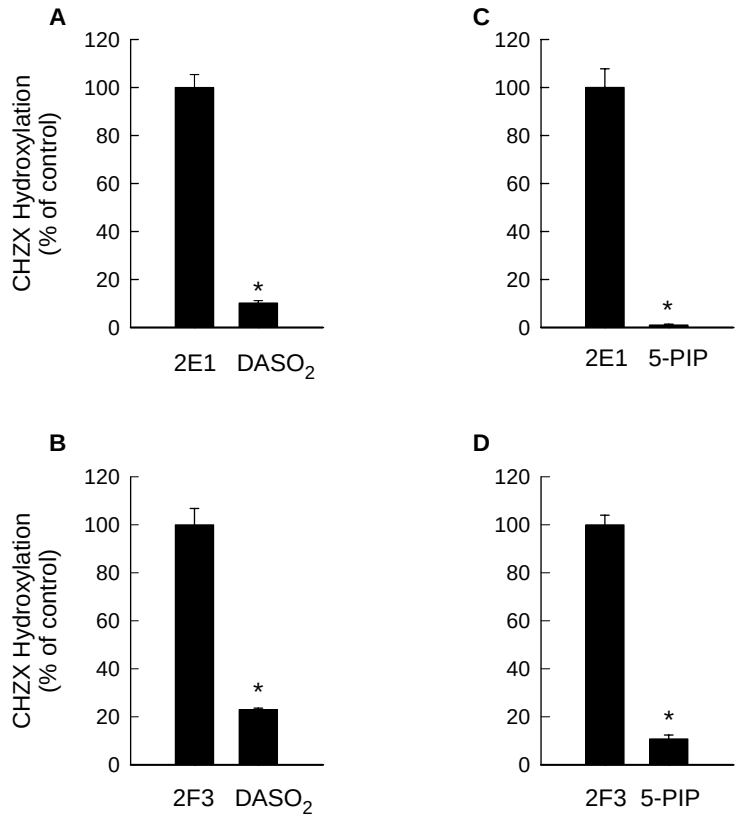

Figure 5

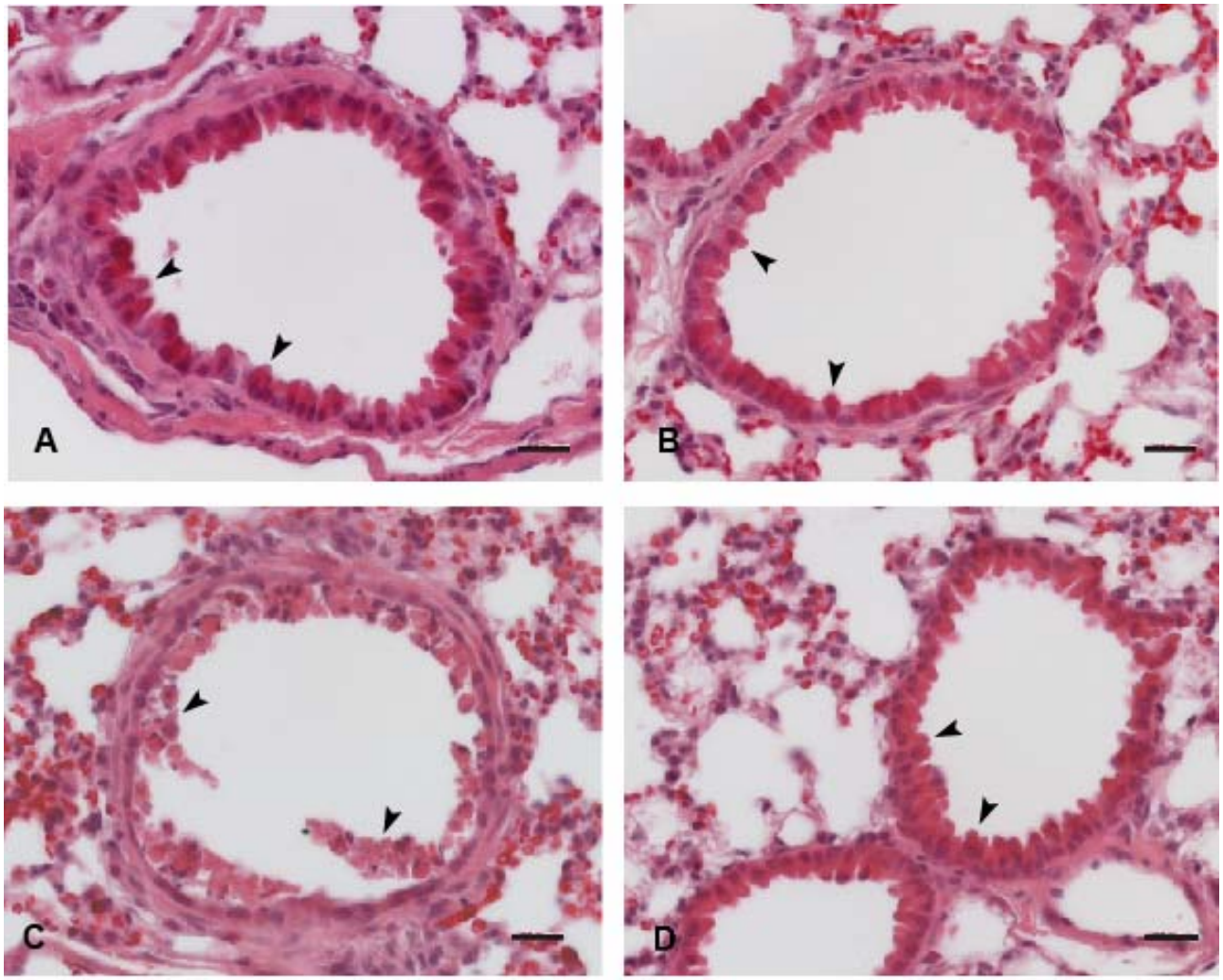

Figure 6

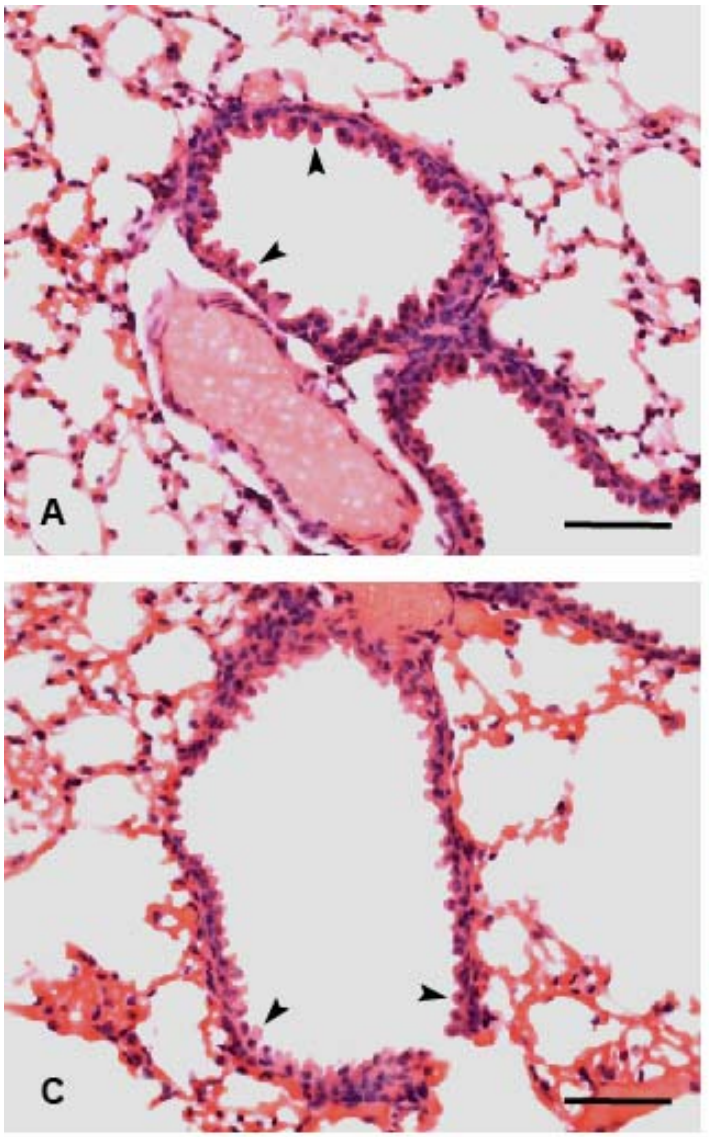

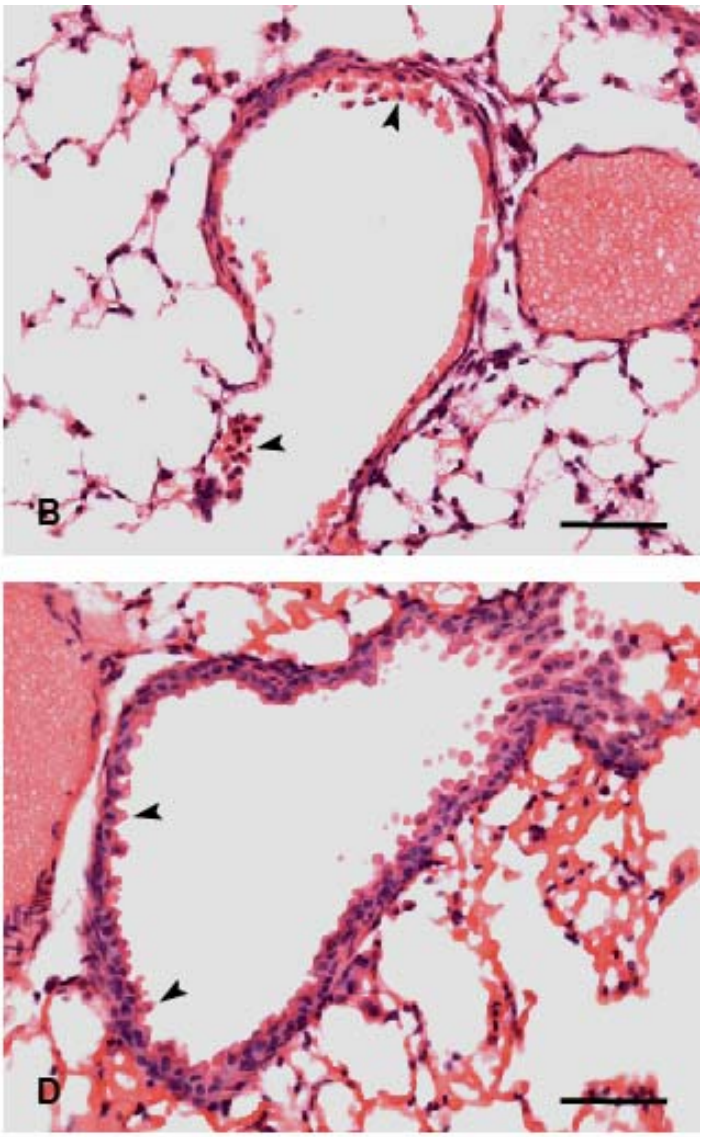

Figure 7

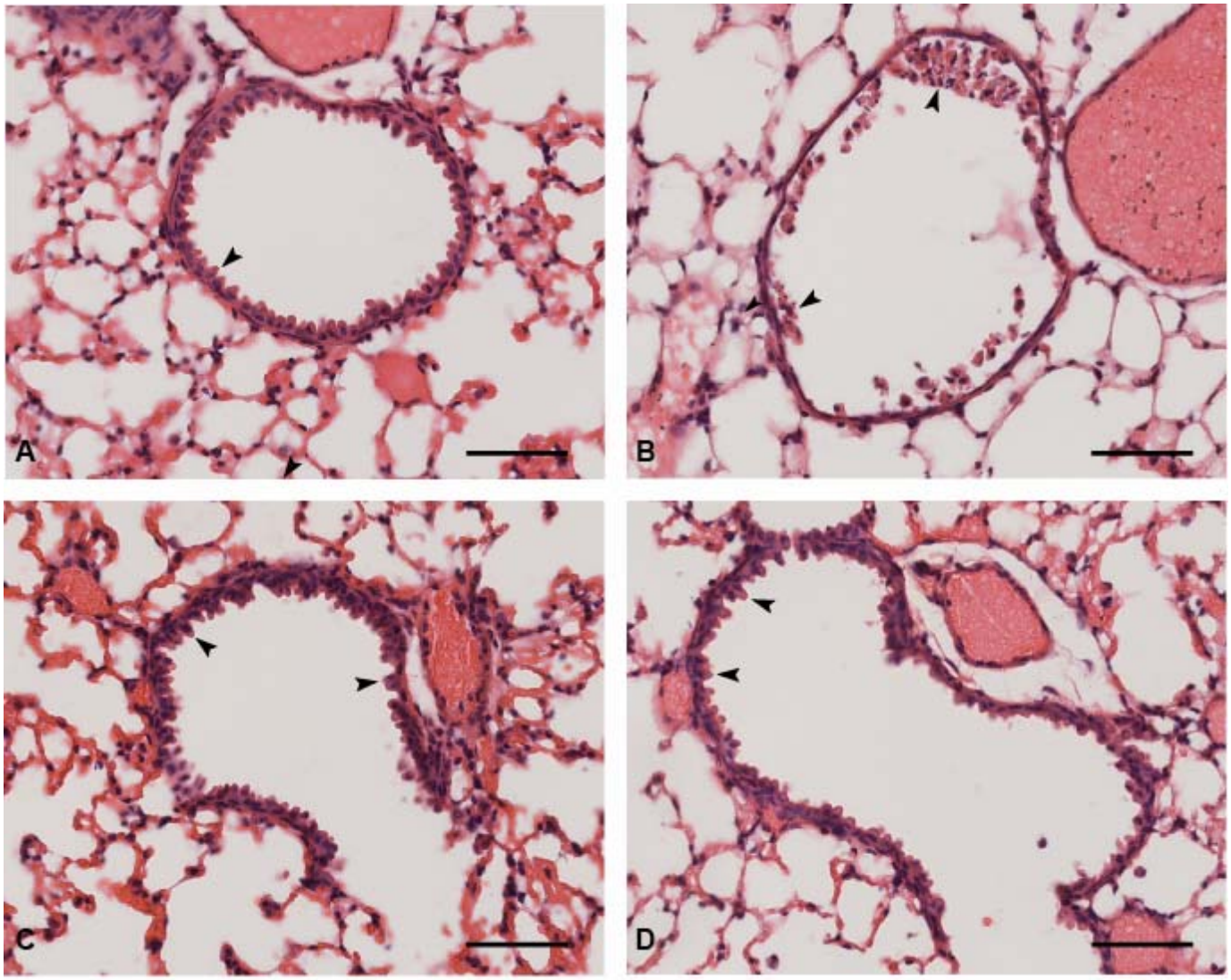

Figure 8